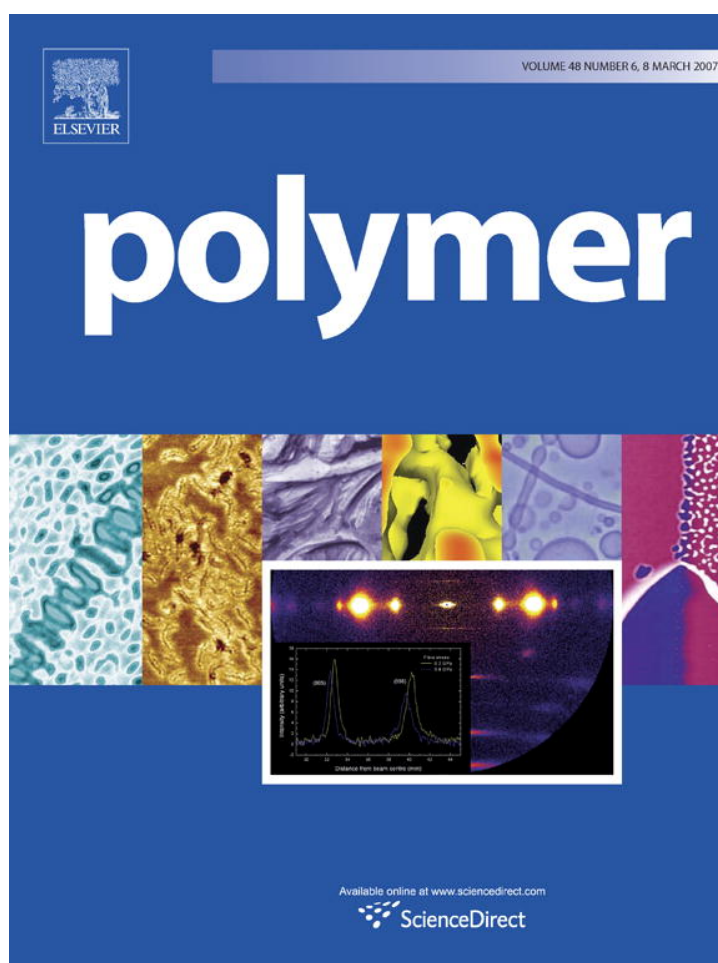


Provided for non-commercial research and educational use only.  
Not for reproduction or distribution or commercial use.



This article was originally published in a journal published by Elsevier, and the attached copy is provided by Elsevier for the author's benefit and for the benefit of the author's institution, for non-commercial research and educational use including without limitation use in instruction at your institution, sending it to specific colleagues that you know, and providing a copy to your institution's administrator.

All other uses, reproduction and distribution, including without limitation commercial reprints, selling or licensing copies or access, or posting on open internet sites, your personal or institution's website or repository, are prohibited. For exceptions, permission may be sought for such use through Elsevier's permissions site at:

<http://www.elsevier.com/locate/permissionusematerial>

# Molecular mechanisms of the chain diffusion between crystalline and amorphous fractions in polyethylene

E.A. Zubova<sup>a,\*</sup>, N.K. Balabaev<sup>b</sup>, L.I. Manevitch<sup>a</sup>

<sup>a</sup> Institute of Chemical Physics, Russian Academy of Sciences, 4 Kosygin Street, Moscow 119991, Russia

<sup>b</sup> Institute of Mathematical Problems of Biology, Russian Academy of Sciences, Pushchino, Moscow Oblast 142290, Russia

Received 4 August 2006; received in revised form 14 December 2006; accepted 15 December 2006

Available online 20 December 2006

---

## Abstract

We revisit the problem of the molecular mechanism of the chain diffusion between crystalline and amorphous fractions in semicrystalline polyethylene (PE). There exists a long-standing controversy on the nature of the topological point defects which diffuse along the chain stems in crystallites and shift the stems. Namely, the conformational (including *gauche* conformations) twist–compression (interstitial-like) and the smooth (soliton-like) twist–tension (vacancy-like) localized defects were offered for this role. However, none of the proposed models for the process could explain all the experimental facts which seemed unclear and contradictory. Moreover, it was discovered recently that in PE samples of uncommon morphology (electron beam irradiated samples, fibers and single crystals) the diffusion process has the activation energy about 3 times less than that in common melt-crystallized samples. No explanation ever followed. We have carried out molecular dynamics (MD) simulation of both the defects in a realistic model of PE crystal and obtained estimates for their formation energies and diffusion coefficients. These estimates together with analysis of available experimental data allow to solve both the problems and to propose models for molecular mechanisms of the observed diffusion processes. The agents of the ‘old’ diffusion process are the smooth twist–tension defects. Shifts in a chain stem of a crystallite in a common sample are initiated at the interface to an amorphous region through extended thermal motion of the chain stem in the amorphous region. If the motion causes a strong pull (with a twist) at the chain stem in the crystallite, such motion produces a smooth defect of twist–tension on this stem. The proposed molecular model conforms with available mechanical experiments if one accepts that the process corresponds to the most low temperature ( $\alpha_1$ ) from the  $\alpha$ -peaks observed. The ‘new’ diffusion process results from diffusion of the conformational twist–compression defects in crystallites. The needed sequence of conformations appears near a crystallite as a result of a quick gamma process. Because the state of the semicrystalline polymer is unstable, the position of the boundary between the crystalline and disordered regions fluctuates so that segments of chains pass from disordered to crystalline state (and vice versa). The conformational defects in disordered region are captured through expansion of the crystalline region where they become stable and diffuse along the chains. Our MD estimate for the activation energy of the process  $E_{act} \leq 8.65$  kcal/mol is in a good agreement with the experimental value 7 kcal/mol. The diffusion coefficients of both the defects are too high to have effect on the statistics of both of these very slow processes. Therefore the statistics of the ‘old’ process is the statistics of strong thermal pulls at chain stems in crystallites, and the statistics of the ‘new’ process is related to the statistics of fluctuations of the position of the boundaries between crystalline and disordered fractions.

© 2007 Elsevier Ltd. All rights reserved.

PACS numbers: 82.35.Lr; 61.72.-y; 61.72.Bb; 61.72.Hh; 02.70.Ns

Keywords: Polyethylene;  $\alpha$ -Relaxation mechanism; Chain diffusion

---

## 1. Introduction

The chain diffusion between crystalline and amorphous fractions is present only in a handful of semicrystalline

polymers, such as polyethylene (PE), isotactic polypropylene, polyvinylidene fluoride, polytetrafluoroethylene, poly(oxy-methylene), poly(ethylene oxide) and several others. The process provides the ultradrawability of these polymers [1]. The most striking draw ratio of 400 is obtained in dry gel films of PE [2], the simplest polymer which always served as a ‘model system’. The presence of the chain diffusion through

\* Corresponding author. Tel.: +7 495 939 7235; fax: +7 495 137 8284.  
E-mail address: [zubova@center.chph.ras.ru](mailto:zubova@center.chph.ras.ru) (E.A. Zubova).

crystallites of PE is verified by direct  $^{13}\text{C}$  NMR experiments in common melt-crystallized samples [3] and in samples of uncommon morphologies: fibers [3], electron beam irradiated samples [4] and even in single crystals [5].

The process of the chain diffusion through crystallites in the samples of uncommon morphologies has the (constant pressure) activation energy 7 kcal/mol – about 3 times less than that in the common melt-crystallized samples (25 kcal/mol). The electron beam irradiation forms crosslinks in amorphous fraction and at chain loops in PE samples (see Ref. [4] and references therein). Consequently, the chains in the amorphous layers of these samples become (to some extent) immobilized – just as disordered fraction (chain loops and chain ends) of single crystals and fibers. So, in the samples with low mobile disordered fraction one can observe a diffusion process different from that in the common samples possessing highly mobile rubber-like amorphous fraction. For brevity sake, these processes will be referred to as ‘L-diffusion’ and ‘H-diffusion’.

The comparison of the NMR data presented in Refs. [3,6] shows that a shift of a chain stem in a crystallite by one  $\text{CH}_2$  unit (half of the chain period) is accompanied by a ‘flip’ of the stem (the turn through  $180^\circ$ ) and so we deal with diffusive ‘screwing’ of the chain stems in crystallites. The flips of the chain stems in crystallites in the H-diffusion process were known since the fifties of the past century [7–9]. The flips showed up in the high-temperature ( $\alpha$ ) dielectric relaxation of slightly oxidized PE [8,10,11]. On the other hand, crystallites and amorphous layers in such samples are connected by ‘through-pass’ chains passing by turns through the crystallites and the amorphous layers. The shifts of these chains must be detectable mechanically.

The  $\alpha$  dielectric loss peak obtained in isothermal scans is uncommonly narrow (its width is about 2 decades), and its shape is very close to the Debye one. The activation energy of the H-process does not practically depend on the mode of sample preparation [12], crystallinity [10], or pressure [13] at available temperatures. So the H-process seems to be very promising for molecular model development. On the other hand, in mechanical experiments the process is generally observed at lower frequencies and looks much broader (see Ref. [14] for detailed comparison). On the samples of different morphologies, one (single crystal mats [15]), two (melt-crystallized bulk specimens: [16,17]) or even three (ultradrawn dry gel films [18] or fibers from branched PE [19]) peaks can be observed.

In 1966 Hoffman et al. [20] developed a series of ‘site’-type phenomenological molecular models of the H-process. He took into account even the possibility of chain twisting. Later, one of the Hoffman’s models was supplemented [21] for explanation of mechanical experiments through the chain diffusion between crystallites and amorphous regions. But this idea has never been common in the explanation of mechanical observations (see reviews [22,23]). The  $\alpha_1$ -peak (at lower temperatures) was assigned to the interlamellar slip [24] or friction at the boundaries of intralamellar mosaic blocks during their slip [22] or rotation (see Ref. [25] and references

therein), and the  $\alpha_2$ -peak (at higher temperatures) – to crystalline deformation. Only after the direct NMR observation of the flips of chains in crystallites [6], several authors began to associate one of the mechanically observed  $\alpha$ -peaks ( $\alpha_1$  [27] or  $\alpha_2$  [26]) with the chain diffusion through crystallites and so to identify one of the mechanical processes with the dielectrically and NMR observed H-process. Kolesov et al. [28] uses this idea of the chain diffusion for the qualitative explanation of the influence of crystal morphology and chain branching on parameters of the unresolved mechanical process.

As regards the physics of the flips and the shifts of chains, it was evident that the chains in PE crystallites did not rotate as a whole, unlike the chains in paraffins [20]. Indeed, the activation energy of the process does not depend on the thickness of crystallites [10]. Hence, a chain in a crystallite may be rotated and shifted only after a passage of some localized topological defect along this chain. There were two hypotheses on the nature of such a defect: it may be an interstitial-like defect including *gauche* conformations [29] or a smooth [30] soliton-like [31] twist–tension (or twist–compression) defect. Both of the defects were supposed to enter a crystallite from the outside, to diffuse along a chain to the opposite end and then to disappear.

The presence of *gauche* conformations and some sequences of *gauche* and *trans* conformations (for example, *gg* and *gtg*) in PE crystallites is confirmed by infrared spectroscopic measurements [32,33], and they are abundant there at high temperatures (see [33] and the comparison between  $^{13}\text{C}$  NMR- and X-ray-determined degree of crystallinity of a PE sample at elevated temperatures ([34], p. 4335–4336)). However, this fact cannot be regarded as a direct proof for the existence of the above-mentioned conformational defects of a definite type (the simplest one is  $tg^+tg^-tg^+t$ ). On the other hand, the presence of the local smooth twists in crystalline stems cannot be unequivocally verified because of technical reasons [35].

The main argument against the idea of the conformational defects was [30] that, as the defects are about 6 or 7  $\text{CH}_2$  groups long, the model cannot explain the drastic change in the dependence of the central temperature (in isochronal scans) on the lamellar thickness at a point of 100 Å. The central temperature of the H-process strongly depends on the chain length in paraffins, while the dependence becomes a weak one in PE samples (when the lamellar thickness is more than 100 Å) – see Fig. 12 in Ref. [20] summing up dielectric and mechanical data on paraffins, single crystal PE mats and bulk PE. The idea of the smooth defects as agents of the process easily explains this fact. Indeed, the valence angles in PE molecule are much more rigid than the torsional ones. Therefore the tension area of the smooth defect is much longer than the twist area and just equals to 100 Å (see Refs. [36,37]). So, chains in paraffins rotate as a whole until they are long enough to form a smooth defect on themselves, whereupon the motion of such defects becomes the mechanism of the chain diffusion. On the other hand, there is no reason why the molecular mechanisms of chain diffusion may not be different in paraffins and PE. Indeed, melt-crystallized PE contains amorphous fraction where the

conformational defects are abundant, and this fact may change the mechanism of the rotation of the chains.

The defects (of whatever type) were supposed to diffuse along the chain stems in crystallites. There were two main models of this diffusion. The statistical model developed in Ref. [38] implied that the defects diffuse freely in a sample as in a single chain. Fitting parameters of the model [38] are the density of the defects and their diffusion coefficient. To fit the experimentally observed dielectric loss curve for the H-process, the diffusion coefficient must be  $2 \times 10^5$ – $2 \times 10^7$  cm<sup>2</sup>/s (depending on temperature) [39], and the diffusion process must be sufficiently non-Einsteinian. For comparison, the diffusion coefficient (at room temperature) of hydrogen in oxygen is 0.7 cm<sup>2</sup>/s, and that of sodium chloride (common salt) in water is  $10^{-5}$  cm<sup>2</sup>/s. No elaboration of the model improves the situation [40]. In 2002 we [41] obtained diffusion coefficient of the smooth twist–tension defect in a simplified MD model of the PE crystal with united atoms (CH<sub>2</sub> groups were replaced by point particles):  $4 \times 10^{-2}$  cm<sup>2</sup>/s, and this must be the upper estimate of the real value. The diffusion coefficient of the conformational defects must be of course less. So, there is no reason to suggest that the diffusion of the defects is non-Einsteinian. It proved to be possible to select physically reasonable values for the density and the diffusion coefficient of the defects to fit experimentally observed central frequency of the H-process [41], but it is impossible to fit the shape of the loss curve without invoking the statistics of their generation which had never been taken into account in the model. In fact, the assumption that the defects can diffuse freely along the chains through loops in crystallites and amorphous regions occupied with entanglements and conformational defects was the weakest point of the model from the outset.

Another approach [42] included the premise that the (conformational) defects come from the amorphous phase where they are in abundance, while their concentration in the crystalline phase is limited. In this case the central frequency of the process is in inverse proportion to the ‘first passage time’ for the diffusing defect and therefore in proportion to the diffusion coefficient. An estimate was made for the diffusion coefficient to fit the experimental frequency of the H-process. It appeared to be about  $10^{-9}$  cm<sup>2</sup>/s at 340 K. This value looks much more reasonable than the estimates made in the framework of the first approach, but this model has its own weak point. Namely, there is no evidence why coming of the defects from outside is not influencing the frequency of the process. All the reasoning is the purely qualitative argument that the conformational defects are ‘abundant’ in the amorphous fraction. But all that one can definitely assert is that there exists a large population of *gauche* conformations and very rapid *trans*–*gauche* transitions in the amorphous fraction. There are no estimates how often the transitions form the needed 5–7 CH<sub>2</sub> groups’ long sequence of conformations which will live long enough to be able to enter a crystallite where this sequence is energetically unfavorable.

So, the choice of a molecular model for the H-process demands the knowledge of either the frequencies of appearance of the defects of both types in crystallites or the diffusion coefficients of the defects in chains of the crystallites. We are

going to obtain estimates for the diffusion coefficients in a realistic MD model of PE crystal. After it is done we can solve what determines the observed rate of the chain diffusion through crystallites: the rate at which the defects enter the crystallites, the time which the defects need to leave the crystallites from the opposite side, or both the processes. The result appeared to be so that made it possible to make choice not only between ‘coming’ and ‘diffusion’ hypotheses but also between smooth and conformational defects. In light of the achieved results we analyze some recent unexpected and unaccounted-for experimental data obtained on PE samples of uncommon morphologies. First, we propose a molecular model also for the L-diffusion process and obtain MD estimate for the activation energy of this process. Further, we explain unusual changes of the activation energy of the  $\alpha_1$ -process observed in dynamic mechanical experiments [43,2] on the H-diffusion. In addition, we explain some hitherto unclear features of the H-diffusion process.

## 2. MD simulation of smooth twist–tension (vacancy-like) and conformational twist–compression (interstitial-like) defects in realistic model of PE crystal

### 2.1. MD model of PE crystal with a point defect on a chain

For interactions between atoms in PE crystal, we have chosen the Amber force field [44] widely used in mathematical modelling in physics, chemistry and biology. Potentials and parameters of interactions between atoms are listed in Table 1. The cell for calculations was a rectangular parallelepiped with periodic boundary conditions imposed in all three directions. The cell contained fragments of 30 infinite PE chains. Fragments of 29 molecules included 200 CH<sub>2</sub> groups in *trans* conformations. The last chain included 199 or 201 CH<sub>2</sub> groups and had a twist–tension or a twist–compression defect. The defect was initially formed as the uniform tension or compression of a chain section from 50 CH<sub>2</sub> groups along the chain

Table 1

Potentials of interactions between atoms in PE crystal (C – carbon, H – hydrogen) – the Amber force field [44]

Valence bond potential:  $U(L) = K_L(L - L_0)^2$   
 C–C:  $L_0 = 1.526$  Å;  $K_L = 310$  kcal mol<sup>-1</sup> Å<sup>-2</sup>  
 C–H:  $L_0 = 1.090$  Å;  $K_L = 340$  kcal mol<sup>-1</sup> Å<sup>-2</sup>

Valence angle potential:  $U(\theta) = K_\theta(\theta - \theta_0)^2$   
 C–C–C:  $\theta_0 = 109.5^\circ$ ;  $K_\theta = 40$  kcal mol<sup>-1</sup> rad<sup>-2</sup>  
 H–C–H:  $\theta_0 = 109.5^\circ$ ;  $K_\theta = 35$  kcal mol<sup>-1</sup> rad<sup>-2</sup>  
 H–C–C:  $\theta_0 = 109.5^\circ$ ;  $K_\theta = 50$  kcal mol<sup>-1</sup> rad<sup>-2</sup>

Torsion angle potential:  $U(\varphi) = K_\varphi(1 + \cos(3\varphi))$   
 X–C–C–X (X = C or H):  $K_\varphi = 0.156$  kcal mol<sup>-1</sup>

van der Waals pair interactions between atoms separated by more than 2 bonds or belonging to different molecules:  $U(r) = \epsilon((R_{\min}/r)^{12} - 2(R_{\min}/r)^6)$   
 $\epsilon_{CC} = 0.1094$  kcal mol<sup>-1</sup>;  $R_{\min,CC} = 3.816$  Å  
 $\epsilon_{HH} = 0.0157$  kcal mol<sup>-1</sup>;  $R_{\min,HH} = 2.974$  Å  
 $\epsilon_{CH} = (\epsilon_{CC} \times \epsilon_{HH})^{1/2}$ ;  $R_{\min,CH} = (R_{\min,CC} + R_{\min,HH})/2$   
 $R_{\text{cut}} = 10.5$  Å



axis by a half-chain period combined with the uniform twist through  $180^\circ$  of the plane of the chain. The last chain also contained no *gauche* conformations. We have assigned the initial velocities of atoms randomly according to the Maxwell distribution for prescribed temperature.

The system evolved according to the Newton equations of motion with additional terms providing the Berendsen barostat (pressure 1 atm) [45] and the collisional thermostat (with the temperature  $T_{\text{ref}}$ ) [46,47]. Interactions between the thermostat and the atoms of the molecular system were modelled by collisions with virtual particles having mass  $m_0$  and velocities  $v_0$  distributed according to the Gaussian law:

$$P(v_0) = \left( \frac{m_0}{2\pi k_B T_{\text{ref}}} \right)^{3/2} \exp\left( -\frac{m_0 v_0^2}{2k_B T_{\text{ref}}} \right),$$

where  $k_B$  is the Boltzmann constant. The collisions were organized as a Poisson random stream of events with the mean frequency  $\lambda$ . Parameters of the thermostat  $m_0 = 1$  a.u. and  $\lambda = 5.5 \times 10^{12}$  Hz provided only minor additional friction (less than 1% of the internal molecular friction) which had no effect on any dynamic characteristic of the system. The equations of motion were integrated using the velocity Verlet algorithm [48]. Step of integration was 0.5 fs.

The chains were packed into the inherent of PE crystal orthorhombic structure with crystallographic parameters  $a = 7.2 \text{ \AA}$ ,  $b = 4.9 \text{ \AA}$ ,  $c = 2.495 \text{ \AA}$ . Before the productive runs the samples relaxed during 200 ps. The samples had enough time to come to the equilibrium size corresponding to prescribed pressure and temperature. For example, at temperature 300 K the crystal cell had dimensions  $a = 7.34 \text{ \AA}$ ,  $b = 4.90 \text{ \AA}$ ,  $c = 2.554 \text{ \AA}$  (the density  $\rho = 1.0183 \text{ g/cm}^3$ ).

## 2.2. Energies of formation of the defects in PE crystal

Three samples of the PE crystal (the ideal one, with a defect of twist–tension and with a defect of twist–compression) were relaxed at different temperatures ( $T = 10 \text{ K}$ ,  $100 \text{ K}$ ,  $300 \text{ K}$ ,  $360 \text{ K}$ ,  $400 \text{ K}$  and  $500 \text{ K}$ ) and constant pressure 1 atm. We found that the shape of the defects changed (see Figs. 1–3).

The defect of twist–tension, although became narrower, kept smooth, while the defect of twist–compression transformed to the conformational one during first 10 ps. The fact that the smooth twist–compression defect in PE is unstable against thermal fluctuations is already known [49]. Hence, an interstitial-like defect providing  $180^\circ$  twist of a PE chain always includes *gauche* conformations. On the other hand, the PE chain is fully extended, and therefore a vacancy-like defect in PE is always smooth. Consequently, only two point defects of needed topology can exist in PE: the smooth twist–tension defect and the conformational twist–compression one. The twist area in the twist–tension defect comprises about 20, and the tension area – 80  $\text{CH}_2$  groups (see Fig. 2) because of the difference between the rigidities of torsional and valence angles, the defect shape being analogous to the one obtained in Refs. [36,37,50].

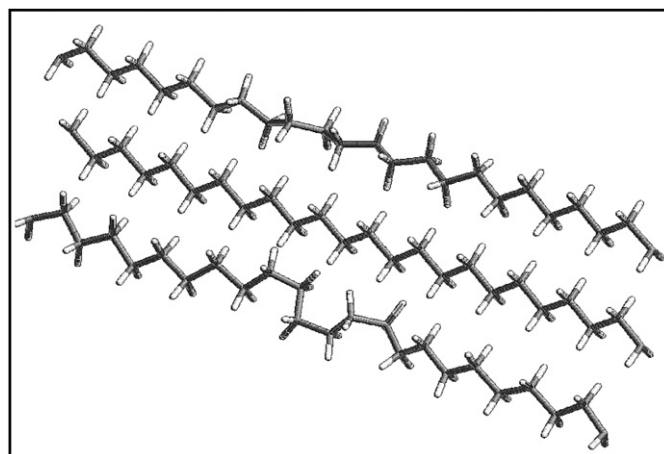


Fig. 1. Appearance of point defects in PE crystal: a smooth twist–tension defect (on the upper chain) and a conformational twist–compression one of the type  $tg^+tg^-tg^+t$  (on the bottom chain) after relaxation of the crystal ('snapshots' at  $T = 10 \text{ K}$ ).

At every temperature  $T$ , we calculated the formation energy of the defect  $E_{\text{form}}$  as time average (on interval 800 ps) of the difference between the energies of a fragment of a chain with the defect and that containing the same number of  $\text{CH}_2$  groups in a defect-free crystal. The different contributions into the energy  $E_{\text{form}}$  were separated.

The results for the lowest temperature  $T = 10 \text{ K}$  (when the thermal fluctuations do not introduce large error in computations) are presented in Table 2. We could not properly trace changes in the energies with temperature because of thermal fluctuations (at  $T = 50 \text{ K}$  and  $100 \text{ K}$  the errors in determination of the total energy are 1 and 3 kcal/mol, respectively). Both defects investigated at  $T = 10 \text{ K}$  correspond to configurations possessing minimal energies, because MD 'annealing' (heating to 300 K and subsequent cooling) has no effect on their energies and their shapes.

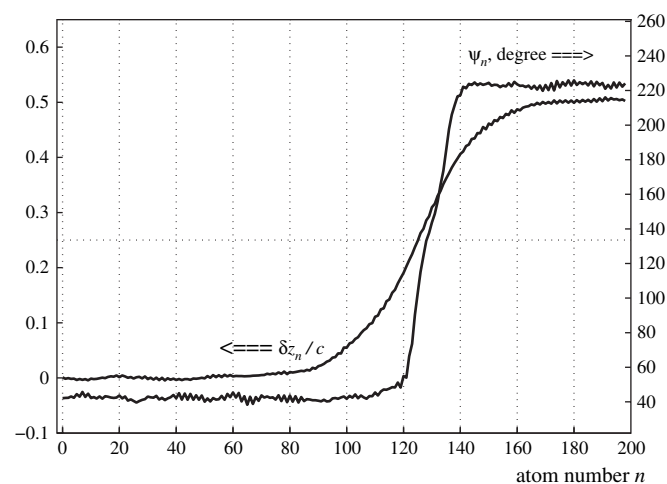


Fig. 2. Shape of the smooth twist–tension defect in a chain of PE crystal at  $T = 300 \text{ K}$ : longitudinal deviations of carbon atoms from their equilibrium positions in an ideal crystal in units of the chain period  $\delta z_n / c$  and angles  $\psi_n$  between  $\alpha$ -axis of the crystal and the projections of the bisectors of the C–C–C angles on the plain orthogonal to the chain axis. Both values are time averages on interval 0.5 ps.

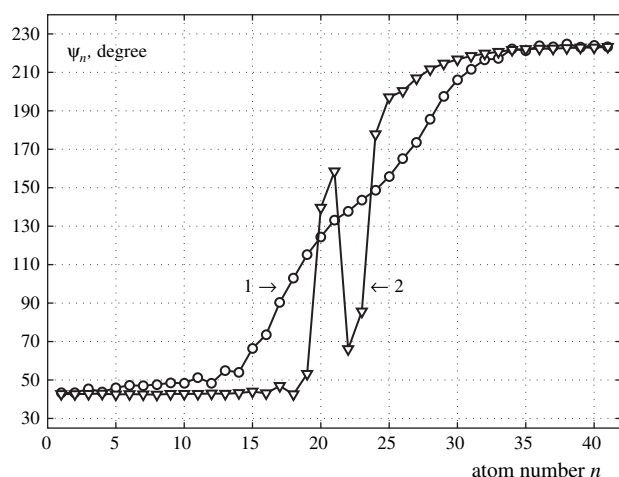


Fig. 3. Comparison of the shape of the smooth twist–tension (line 1) and the conformational twist–compression of the type  $tg^+tg^-tg^+t$  (line 2) defects at  $T = 300$  K: the angles  $\psi_n$  (see caption of Fig. 2) displayed on a shorter portion of the chain. Every point shows the time average on interval 0.5 ps.

The values listed in Table 2 are the upper estimates of the real values – first, because of thermal expansion of the crystal at experimental temperatures, and second, because we have an ideal crystal with infinite chains, which is never the case in real PE. For understanding of the results presented in Table 2 one has to keep in mind that the van der Waals interactions are repulsive even in an isolated chain. In addition, when the chains collect into a crystal, they shrink. The total energies of the defects are close, but the balance of contributions is quite different for the defects. The energy of angles and bonds of the first chain containing the smooth twist–tension defect is very high (24.88 kcal/mol), while the local elongation of the

Table 2

Formation energies of a smooth twist–tension and a conformational twist–compression (of the type  $tg^+tg^-tg^+t$ ) defects in PE crystal at temperature  $T = 10$  K and pressure 1 atm

Energy	Smooth twist–tension	Conformational twist–compression of the type $tg^+tg^-tg^+t$
$\delta U^{\text{tot}}$	$28.33 \pm 0.03$	$25.86 \pm 0.03$
$\delta U_{\text{vW}}^{\text{tot}}$	$15.77 \pm 0.07$	$16.90 \pm 0.07$
$\delta U^{(1)} + \delta U_{\text{vW}}^{(1)-(s)}$	$23.81 \pm 0.04$	$20.50 \pm 0.04$
$\delta U^{(1)}$	$14.41 \pm 0.04$	$11.21 \pm 0.04$
$\delta U_{\text{vW}}^{(1)}$	$-10.470 \pm 0.007$	$10.047 \pm 0.007$
$\delta U_{\text{angle-bond}}^{(1)}$	$24.88 \pm 0.04$	$1.16 \pm 0.04$
$\delta U_{\text{vW}}^{(1)-(s)}$	$9.41 \pm 0.014$	$9.29 \pm 0.014$
$\delta U^{(s)}$	$4.51 \pm 0.05$	$5.36 \pm 0.05$
$\delta U_{\text{vW}}^{(s)}$	$16.83 \pm 0.07$	$-2.44 \pm 0.07$
$\delta U_{\text{angle-bond}}^{(s)}$	$-12.32 \pm 0.09$	$7.80 \pm 0.09$

The full energy of a defect  $\delta U^{\text{tot}}$  consists of the (additional) energy of van der Waals interactions  $\delta U_{\text{vW}}^{\text{tot}}$ , the energies of angles and bonds of the first chain containing the defect  $\delta U_{\text{angle-bond}}^{(1)}$  and the energies of angles and bonds of the rest of the sample  $\delta U_{\text{angle-bond}}^{(s)}$ . One can also divide the van der Waals interactions  $\delta U_{\text{vW}}^{\text{tot}}$  into the interactions in the first chain  $\delta U_{\text{vW}}^{(1)}$ , the ones in the rest of the sample  $\delta U_{\text{vW}}^{(s)}$  and the ones between the first chain and the rest of the molecules  $\delta U_{\text{vW}}^{(1)-(s)}$ . The full additional energy in the first chain is  $\delta U^{(1)}$ , in the rest of the sample –  $\delta U^{(s)}$ , the additional energy of interaction between the first chain and the rest of the molecules is  $\delta U_{\text{vW}}^{(1)-(s)}$ . The energies are in kcal/mol. We also indicate the standard mean square deviation, regarding the averages obtained on independent pieces of one trajectory as independent measurements of the value.

chain is favorable for the van der Waals interactions in it ( $-10.47$  kcal/mol) and the appeared free space allows the neighboring chains to relax their tense in angles and bonds ( $-12.32$  kcal/mol). The imperfection in the crystal adds a large additional value to the van der Waals interactions of the rest molecules in the sample (16.83 kcal/mol). The energy balance for the conformational twist–compression defect is quite the opposite. The defect adds a very little value to the energy of angles and bonds in the first chain (1.16 kcal/mol) because the twist here is ‘conformational’ and therefore cheap. But the contraction of the first chain is unfavorable for the van der Waals interactions in it (10.047 kcal/mol). Moreover, the ‘swelling’ of the first chain results in local perturbation of the neighboring molecules ( $\delta U_{\text{angle-bond}}^{(s)} = 7.80$  kcal/mol) and their slight elongation which leads to a little better situation with the van der Waals interactions in them ( $-2.44$  kcal/mol). Although the conformational twist–compression defect has a little less energy than the smooth twist–tension one, we have to remember that there cannot exist a conformational twist–tension defect in a PE chain and therefore an outward rotation with a pull at a chain stem in a crystallite may result only in a smooth (if any) twist–tension defect injection.

Let us compare our estimates with those of earlier works [30,29,51,37,49,52]. First of all, our estimates are made at constant pressure, while the molecular mechanics (MM) minima of the listed works are to be compared with the constant volume experimental value. The experimental constant pressure activation energy of the  $\alpha$  process in PE is 24.9 kcal/mol, while the constant volume one is  $19.4 \pm 0.5$  kcal/mol [13]. The earliest works [30,29] give the values 11.8 and 10.5 kcal/mol, for the conformational (of the type  $tg^+tg^-tg^+t$ ) twist–compression and the smooth (in a chain consisting of 22  $\text{CH}_2$  groups) twist–tension defects, respectively. Ten years later the values are 11.77 and 21.12 kcal/mol [51], the estimates being made in a chain consisting of 60  $\text{CH}_2$  groups. After the next 10 years Zhang reported the estimates 22.7 kcal/mol [37] and 16.7 kcal/mol [49] for the smooth twist–tension defect in a chain consisting of 100  $\text{CH}_2$  groups. Mowry and Rutledge [52] found 50 conformational twist–compression defects possessing the needed topology and energy ranging from 11 to 25 kcal/mol. The cheapest defects of the type  $tg^+tg^-tg^+t$  have the formation energy of about 11 kcal/mol.

Apropos of this, we are to note that MM estimates have the disadvantage of arbitrary choice of the sizes of the rigid lattice in which the chain with a defect is placed. The lattice must be sufficiently expanded to provide convergence of the minimization procedure. In addition, in the rigid lattice the neighboring chains have no possibility to adjust themselves to the defect. In our MD estimates the sizes of the sample exactly correspond to the used standard force field, because the sample relaxes before the productive runs, and the neighboring chains are mobile. Our analysis shows that for the conformational twist–compression defect of the type  $tg^+tg^-tg^+t$  the deformation of the chain containing the defect costs only 11.21 kcal/mol, while the van der Waals interactions with the crystalline environment cost 9.29 kcal/mol, and the deformation of this environment – 5.36 kcal/mol. One can see that the perturbation of

the crystal around the defect is not small. Comparing with the value 11 kcal/mol for the conformational twist–compression defect of the same type from Refs. [29,51,52], we can suggest that practically all the energy of the defect in these works originated from the deformation of the chain with a defect. In contrast with this, the smooth twist–tension defect can form only in a crystalline environment: the region of smooth deformation can be localized only if the energy of van der Waals interactions with the neighboring chains is close to the energy of deformation of the chain with a defect. Therefore the cited MM estimates in long chains are much closer to our value.

### 2.3. Diffusion coefficients of the defects

The point defects placed in a chain of the crystal do not stay at rest at elevated temperatures; they execute a diffusive motion along the chain ( $Z$ -axis). The displacement of these topological defects is connected with the displacement of the center of mass of the chain where they have been placed as

$$Z_{\text{def}}(t; t_0) = \mp N(Z_{\text{cm}}(t + t_0) - Z_{\text{cm}}(t_0)).$$

Here,  $t + t_0$  and  $t_0$  are the current and the initial time moments,  $Z_{\text{cm}}$  –  $Z$ -coordinate of the center of mass of the periodic fragment of the chain with the defect,  $N$  is the number of  $\text{CH}_2$  groups in fragments of chains without defect ( $N = 200$ ). Recall that the cell for calculations contains fragments of 30 infinite chains; periodic boundary conditions are imposed in all three directions.

We traced  $Z_{\text{cm}}$  during 800 ps. The displacement  $Z_{\text{cm}}$  of a chain without defect is very small. The mean square displacements  $\langle Z_{\text{def}}^2(t; t_0) \rangle_{t_0}$  for the smooth twist–tension and conformational twist–compression defects are shown in Figs. 4 and 5 as functions of time  $t$  for different temperatures.

One can see that the smooth twist–tension defect is much more mobile than the conformational twist–compression one, and in the temperature diapason 300–400 K there is no noticeable temperature dependence of the diffusion coefficient of the smooth twist–tension defect while this is not the case for the conformational twist–compression defect. We have also to mark that different realizations of the diffusion process (at the same temperature) for the conformational twist–compression defects differ widely in the slopes of the lines. The reason is that the defects change from one sequence of conformations to another in the process of motion, and their length varies too. Therefore, in case of the conformational twist–compression defects, we used 16 realizations for every temperature to also obtain ensemble average values. For the smooth twist–tension defect we used 3 realizations. The chosen number of realizations is enough to guarantee for the order of the values obtained, which, as we will see, is enough for our goals.

The diffusion coefficient of the smooth twist–tension defect in the temperature diapason 300–400 K appeared to be  $D_s$  (300–400 K)  $\sim 2 \times 10^{-3} \text{ cm}^2/\text{s}$ . Recall that the diffusion coefficient of the smooth twist–tension defect in the model with united atoms is  $4 \times 10^{-2} \text{ cm}^2/\text{s}$  [41]. The obtained value  $2 \times 10^{-3} \text{ cm}^2/\text{s}$  lies between the values characteristic for gases

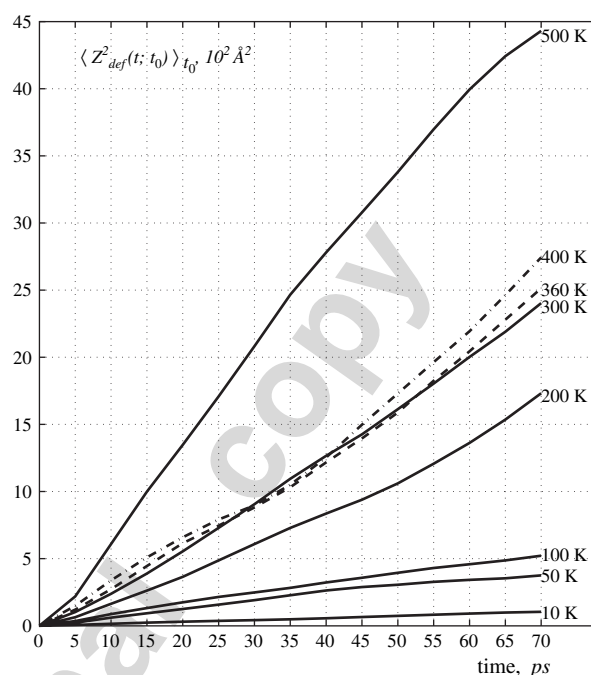


Fig. 4. The mean square displacement of the smooth twist–tension defect as function of time  $t$  at different temperatures. The time averaging was performed during 800 ps along the trajectory of one defect.

and the ones for liquids; for defects in solids it seems very high. But one has to keep in mind that these defects are in fact soliton-like excitations, and so nearer to waves (like phonons) than to common defects (like dislocations) in solids.

The estimates for the conformational twist–compression defect are  $D_c$  (300 K)  $\sim 10^{-6} \text{ cm}^2/\text{s}$  and  $D_c$  (400 K)  $\sim 10^{-5} \text{ cm}^2/\text{s}$ .

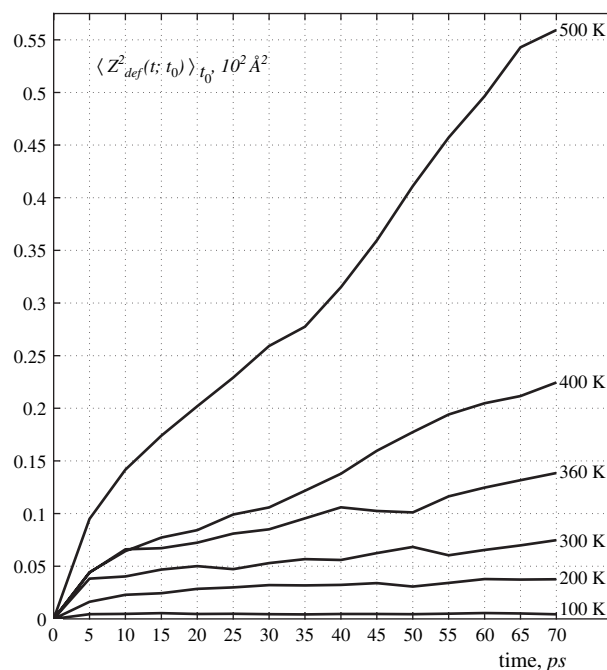


Fig. 5. The mean square displacement of the conformational twist–compression defect as function of time  $t$  at different temperatures. The time averaging was performed during 800 ps along the trajectory of one defect.

#### 2.4. Barriers to propagation along the chain for the defects

Let us examine the diffusion process in more detail. Let us suppose that the displacement of a defect by one CH<sub>2</sub> group is an activation-type process. Then the probability (per time unit) that the defect moves to the right (left) is  $p = q = (1/2\tau_0)\exp(-(\Delta E/kT))$ . Here  $k$  is the Boltzmann constant,  $T$  – temperature,  $\tau_0$  is the time, during which the defect necessarily changes its position at the infinitely high temperature. Then the probability that the defect remains unmoved during time  $\tau_0$  at finite temperature  $T$  is  $r\tau_0 = 1 - p\tau_0 - q\tau_0 = 1 - \exp(-(\Delta E/kT))$ . The difference equation for the probability  $w_z(t)$  to find the defect at the position  $z$  ( $z = nc/2$ ,  $c$  is the chain period,  $n = 0, \pm 1, \pm 2, \dots$ ) at the time moment  $t$  ( $t = m\tau_0$ ,  $m = 0, \pm 1, \pm 2, \dots$ ) takes the form

$$w_z(t + \tau_0) = \tau_0 p w_{z-1}(t) + \tau_0 q w_{z+1}(t) + \tau_0 r w_z(t)$$

Except for the last term, this equation describes a discrete model of the common diffusion (when a particle necessarily moves to the right or to the left after time interval  $\tau_0$ ). Substituting  $p$ ,  $q$  and  $r$  we come to the equation

$$w_z(t + \tau_0) - w_z(t) = \frac{1}{2} \exp\left(-\frac{\Delta E}{kT}\right) (w_{z-1}(t) + w_{z+1}(t) - 2w_z(t))$$

which after transition to continuum approximation becomes the common diffusion equation

$$\frac{\partial w(z, t)}{\partial t} = D \frac{\partial^2 w(z, t)}{\partial z^2},$$

with the only difference that the diffusion coefficient depends on barrier energy  $\Delta E$ :

$$D = \frac{c^2}{8\tau_0} \exp\left(-\frac{\Delta E}{kT}\right).$$

The knowledge of this dependence allows one to estimate the barrier energy  $\Delta E$  for both types of defects. Because the diffusion coefficient for the smooth twist–tension defect does not depend on the temperature in the diapason 300–400 K, one can conclude that the defect propagates along the chain practically without barrier as we did expect for this soliton-like excitation. The barrier for the conformational twist–compression defect (as estimated from the difference between  $D_c$  (300 K)  $\sim 10^{-6}$  cm<sup>2</sup>/s and  $D_c$  (400 K)  $\sim 10^{-5}$  cm<sup>2</sup>/s) appears to be equal to  $\Delta E_c \sim 5$  kcal/mol. The defects change their shape, as well as the number and the order of conformations during their motion, therefore our estimate is a statistical one. Molecular mechanics in a similar model [52] gives a very wide diapason from 4 to 15 kcal/mol for the barrier energies for different defects.

### 3. The main result of MD simulations: what determines the rate of the chain diffusion between fractions

The diffusion process cannot be caused by point structural defects born in crystallites themselves. Indeed, because of

topological charge, the defects can appear there only in pairs: one of twist–tension plus one of twist–compression. The formation energy of a pair (our MD estimate is (28.3 + 25.9) kcal/mol) is twice as high as the observed activation energy of the H-diffusion process and about 6 times as high as that of the L-diffusion. Therefore, the ‘agents’ have to enter from outside and in the last case of the L-diffusion to enter in a very special way. The mechanism of such entering has never been discussed before.

The problem is that the smooth twist–tension defect exists only in a chain placed in a crystal environment (a smoothly twisted area of a chain may be localized only if the chain is in a crystal form). The similar situation is for the conformational twist–compression defects. Although they can exist in amorphous fraction, they cannot persist long in it because of the presence of very rapid gamma processes causing conformational changes. It is the crystalline environment that makes the conformational defects stable. Accordingly, the diffusion of both types of point defects makes sense only in a chain stem belonging to a crystallite. When the defects reach the borders of crystallites (chain loops, chain ends and beginnings of amorphous parts of through-pass chains), they disappear. How soon does it happen?

Our MD simulations give an answer. The answer is: both defects run through crystallites (shifting and flipping the chain stems in the crystallites) practically instantly in comparison with the observed periods of the processes. Indeed, let us find the time that a defect just entered a crystallite remains in it before leaving it from the opposite side. As the simplest upper estimate of the value we may use the average first passage time for one-dimensional motion. Namely, if a diffusing particle (diffusion coefficient  $D$ ) starts at  $Z = 0$  and is adsorbed at  $Z = L$  (the boundary of segment  $(0, L)$  at  $Z = 0$  is transparent, at  $Z = L$  – adsorbing), its most probable lifetime is  $\tau = L^2/(6D)$ . Accepting  $L = 300$  Å and  $T = 300$  K, we obtain for the conformational twist–tension defect  $\tau_c = 1.7 \times 10^{-6}$  s and for the smooth twist–tension defect  $\tau_s = 0.8 \times 10^{-9}$  s. The experimental central frequency of the chain diffusion between fractions is 6 Hz for common melt-crystallized samples, and about 10 Hz for single crystals (see Fig. 6, lines 3, 8, and 9). Comparing with the values  $\tau_c$  and  $\tau_s$ , we see that the experimental frequencies of chain shifts in crystallites are the frequencies at which point defects enter the chains to leave them at the opposite side – the frequencies of injection of the defects.

In this case, in experimental dependence of the central frequency of the process on temperature  $f_0 = F \exp(-E_{act}/kT)$ , the activation energy  $E_{act}$  must be equal to the energy needed to obtain a defect in a chain stem in a crystallite.

## 4. Defects and processes

### 4.1. Molecular mechanism of the H-diffusion

The formation energies of the smooth twist–tension and the conformational twist–compression defects are equal to 28.3 and 25.9 kcal/mol, respectively (Table 2), the experimental value being about 25 kcal/mol [53]. As we already mentioned before, both the estimates are the upper ones because



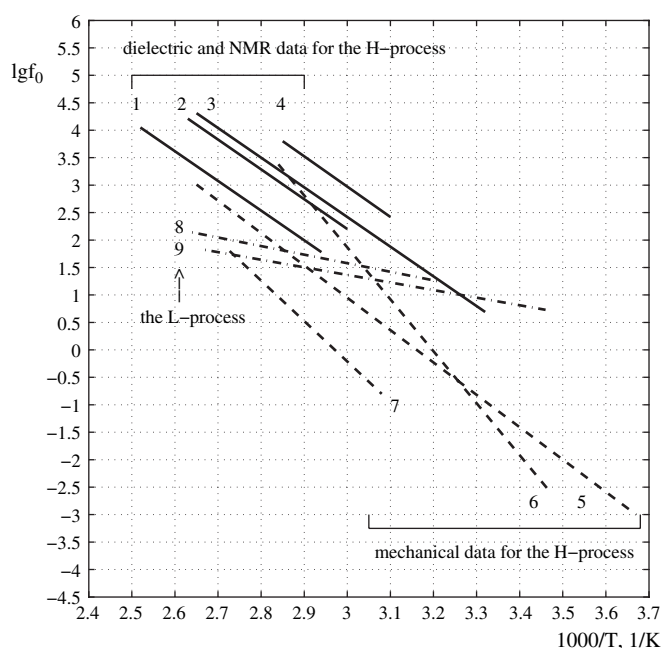


Fig. 6. Central frequencies of the chain shifts and flips in crystallites of different PE samples as observed in dielectric, NMR and mechanical experiments. Solid lines represent dielectric data [10] (lines 1, 2, and 4) and [53] (line 3): line 1 – sample A94-1CE, pressure crystallized and slowly cooled under pressure (96% crystallinity); line 2 – sample A92-1, compression molded and slowly cooled under pressure (76% crystallinity); line 4 – sample A94-1Q, quenched compression molded film (62% crystallinity); line 3 – sample which is melt-pressed and slowly cooled under pressure similar to sample A92-1. NMR results for frequencies of chain shifts [3] and flips [6] fall on line 2. Dashed lines correspond to mechanical measurements: line 5 represents the  $\alpha_1$  process resolved from the  $\alpha_2$  one in Ref. [24] on the basis of the data from work [16]; line 6 – unresolved  $\alpha$  peak obtained on a sample prepared by conventional injection molding [55]; line 7 – unresolved  $\alpha$  process in slowly cooled high density PE sample [28]. We also show the ‘7 kcal/mol’-process observed in NMR experiments on PE samples of uncommon morphologies: line 8 – in single crystals [5], line 9 – in electron beam irradiated melt-crystallized sample [4]. NMR estimates for fibers [6] fall near line 8.

they are made at a very low temperature and in an ideal crystal. We cannot definitely select the ‘right’ defect because the magnitude of the shift is unknown and may be different for the defects. Both defects can provide the process if they emerge in the crystalline fraction near the boundary with the amorphous one. This manner looks quite natural for the smooth twist–tension defect. It can be created by extended modes of thermal motion of the amorphous part of a through-pass chain, if this motion causes rotation and pull at the crystalline part of this chain. And it is this motion that initiates the process because the H-diffusion is absent (or has central frequencies lower than 10 Hz at every temperature) in samples with amorphous fraction cross-linked by electron beam irradiation [4]. On the other hand, one can hardly imagine successful pushing (with rotation) of such a flexible chain into the crystal with subsequent creation of the conformational twist–compression defect. It is much easier for the chain to bend under the action of such a push. Therefore the agents of the H-diffusion are the smooth twist–tension defects.

The H-process is initiated at the boundary between fractions by extended modes of thermal motion of the amorphous part of a through-pass chain entering a crystallite. The motion includes a ‘twisted’ pull at the chain stem in crystallite. This pull generates a smooth twist–tension defect on the chain stem belonging to the crystallite. The smooth twist–tension defect reaches the opposite side of the crystallite by dint of diffusive motion very quickly, and rotates and shifts the chain stem. Then it dies pulling the adjacent (to this remote side) amorphous part of the chain. The net result is a shift (plus rotation) of the chain through the crystallite. The activation energy of the process consists of the formation energy of the defect in a crystallite (the main part) and the energy required for accompanying shifts of amorphous parts of the chain. This last contribution may be different for samples with different thermal histories and consequently with different morphologies. Therefore the observed activation energies may slightly differ, which is the case. The formation energy of the defect is high and therefore the event must be rare, and the process must be very slow, which is the case as well.

#### 4.2. Molecular mechanism of the L-diffusion

The situation with the second diffusion process is more difficult. The L-process was observed in three independent  $^{13}\text{C}$  NMR experiments investigating the chain diffusion through crystallites in electron beam irradiated semicrystalline samples [4], fibers [6] and single crystals [5]. The process showed a very uncommon combination of a very low central frequency and a very low activation energy: 7 kcal/mol (see lines 8 and 9 in Fig. 6, compare with lines 1–4 corresponding to the H-process). With so little expenditure of energy, it is impossible to create any point defect, but there is a chance to ‘squeeze’ a conformational twist–tension defect (already formed by gamma process near a crystallite) into the chain stem of the crystallite. If the defect came from a chain stem placed in vacuum, the activation energy would equal to (see Table 2)  $E_{\text{act}}^{(\text{vac})} = \delta U_{\text{vW}}^{(1)-(s)} + \delta U^{(s)} + n\Delta E_c = (9.29 + 5.36 + 5n)$  kcal/mol. The first two contributions arise because one needs to build the defect into the crystal. The last term is included because the conformational defect is to cross at least  $n$  barriers in its motion across the boundary between fractions along the chain ( $n$  is the width of the conformational defect, the minimal value of  $n$  is equal to 5–7). So the activation energy seems to be too high.

But the defect is on a chain placed not in vacuum but in a disordered fraction. It is an end of a chain in a fiber, or a loop of a chain in a single crystal, or an immobilized amorphous fraction (in electron beam irradiated samples). The state of the solid polymer is unstable. The boundary between the crystalline and the less ordered parts of chains fluctuates so that segments of the chains pass from disordered to crystalline fractions (and vice versa). If a conformational twist–compression defect forms in the disordered fraction and then (because of the motion of the boundary between the fractions) turns out to be in the crystalline fraction, it cannot decay and must diffuse in the crystalline stem. Such a way of transfer of conformational defects into crystalline regions must be much

cheaper than entering the crystallites from the outside because the expansion of a crystalline region is energetically favorable: our simulation [54] showed that the gain in energy for one CH<sub>2</sub> group is about 1.2 kcal/mol. The size of fluctuating area must be not less than 5 CH<sub>2</sub> groups along the crystal axis (the length of the shortest conformational defect), so that the minimal gain in energy is –6 kcal/mol. The penalty for transferring the defect into the crystal must be less than (see Table 2)  $\delta U_{vw}^{(1)-(s)} + \delta U^{(s)} = 14.65$  kcal/mol. So the activation energy of the process  $E_{act} \leq (-6 + 14.65)$  kcal/mol = 8.65 kcal/mol. This MD estimate is in very good accordance with the observed activation energy.

In summary, the L-diffusion process is caused by diffusion in crystalline stems of the conformational twist–compression defects. The needed sequence of conformations (for example, the shortest and the cheapest one is  $tg^+tg^-tg^+t$ ) is formed in the disordered fraction (loops and ends of chains or immobilized amorphous phase) as a result of a quick gamma process. Then the defect is captured by a crystalline region through the fluctuations of the boundary between the crystalline and disordered regions. Getting into a crystalline region, the defect cannot decay and quickly diffuses along the stem. Similarly to the smooth twist–tension defect, the conformational twist–compression one rotates and translates the stem. The only difference is that the conformational twist–compression defect translates the chain in the same direction it moves itself, while the smooth twist–tension defect in the opposite direction. On the opposite side of the crystalline area the defect is quickly destructed by the same gamma process. In the process of motion the defect may change the number of *gauche* conformations, becomes longer or shorter. We saw such changes in our simulations at elevated temperatures. But the crystalline structure does not allow the defect to change its topology. Therefore the defect safely delivers a CH<sub>2</sub> group to the opposite side of the crystalline area. The formation of the needed (long enough) sequence in the proper place at the proper time cannot be very often, so the process must be rare (and it is very rare – see Fig. 6). The rare ‘occasion’ and the cheap ‘delivery’ result in contradictory properties of the observed L-diffusion: low central frequency and low activation energy.

#### 4.3. Conditions of observation of the different diffusion processes

The H-diffusion is absent or slower than 5 Hz at all accessible temperatures in the samples of uncommon morphology. In the framework of the proposed hypothesis one can easily understand the reason. Indeed, there is no genuine rubber-like amorphous fraction in single crystals and in fibers, and when the amorphous fraction is cross-linked by electron beam irradiation, it is also not able to perform extended movements which can pull chains out of crystallites. In the absence of the quicker H-diffusion, one can observe the L-diffusion because the formation of the conformational twist–compression defects near the crystallites and the fluctuations of the boundaries between fractions are yet possible.

## 5. Explanation of some hitherto unclear features of the H-diffusion process

### 5.1. Dielectric data: dependence of central frequency on pressure and mode of sample preparation

The central frequency (at given temperature) of the H-process strongly depends on thermal history of the samples. In quenched samples with low crystallinity and very thin crystallites the process goes 6 times quicker, while in pressure crystallized samples (96% crystallinity) – 6 times slower than in common PE samples (Fig. 6). This feature was interpreted as the dependence on the thickness of crystallites. The thicker is a crystallite, the longer it takes for a defect to get to the opposite side. This consideration is valid in both interpretations of the ‘diffusive barrier crossing’ [30] for the smooth twist–tension defect and the ‘first passage time’ [42] for the conformational twist–compression one. Both these models after proper choice of the fitting parameters (the scattering probability and the diffusion coefficient, respectively) seem to qualitatively explain the dependence observed. But, as we have seen, both defects diffuse so quickly that both the models are wrong. So the reason of the observed dependence of the central frequency on thermal history of the samples must be different. Furthermore, the increase in pressure to 4 kbar makes the process 100 times slower – keeping its activation energy [13]. This feature has never got any explanation. Both facts look quite natural in the framework of our hypothesis. Indeed, the central frequency must depend on the state of the amorphous fraction causing the pulls at chains in crystallites. In the quenched samples with large amount of loose amorphous fraction the process must go quicker, while in the pressure crystallized samples where the amorphous fraction is scarce and restricted in motion – slower. The pressure application evidently squeezes the amorphous fraction and therefore sufficiently slows the process.

### 5.2. Mechanical data: which of mechanical $\alpha$ -peaks results from the H-diffusion

We have already mentioned in Section 1 that the process of the chain diffusion through crystallites has never been common in interpretation of mechanical results. But none of the proposed explanations of the mechanical  $\alpha$ -processes can cause dielectric  $\alpha$  relaxation because none of them includes rotation of chains inside crystallites. One could suppose that the ‘dielectric’  $\alpha$  process is located at higher frequencies and has nothing to do with the mechanical  $\alpha$ -peaks. But let us compare some recent results on the dependence of the central frequency of the mechanical process on the temperature (isochronal experiments; unresolved peak): lines 6 [55] and 7 [28] in Fig. 6. Both these samples were more or less ‘common’, but line 6 shows practically dielectric frequencies while line 7 goes indeed much lower. Line 5 was obtained much earlier [24] and represents the  $\alpha_1$  peak separated from the rest of the  $\alpha$ -peaks by rheological methods. Unfortunately, no one carries out the separation now, but it is seen directly from

master curves that the frequencies of the mechanical process mostly agree with the dielectric results (see, for example, Fig. 3 of Ref. [34] and Fig. 7 of Ref. [43]). The discrepancy seems to result from two causes: first, from the difference in sample preparation which leads to different states of the amorphous fraction; and second, from the influence of the other  $\alpha$  processes on the unresolved curve.

Recently, the wider diapason of frequencies became available in mechanical experiments. In work [34] the master curve between  $10^{-6}$  and  $10^8$  Hz was constructed, and no peak between two  $\alpha$ -peaks and two  $\gamma$ -peaks has been discovered. Therefore, either the diffusion of chains between amorphous and crystalline fractions is not active mechanically, or it corresponds to one of the  $\alpha$ -peaks. We think that the dielectrically observed chain flips in crystallites (H-process) manifest itself mechanically in common samples as the  $\alpha_1$  process: the cheapest one having the same activation energy and possessing the highest central frequency from the mechanical  $\alpha$  processes.

Its common assignment is the friction between mosaic blocks of lamellar platelets by their slip [22] or rotation (see Ref. [25] and references therein). But the results of dynamic mechanical experiment [43] on melt-extruded highly anisotropic films cannot be convincingly interpreted in such a way. Let us show it. The melt-extruded film is composed of thin lamellae uniaxially oriented with the  $c$ -axis parallel to the machine direction which lies in the film plane. Between the lamellae are located thin amorphous layers. The types of the blocks' slips caused by mechanical oscillations applied at orientations  $0^\circ$  and  $90^\circ$  with respect to the machine direction have to be quite different. There is no reason why these slips must have equal activation energies. But the activation energies are 28.2 and 28.9 kcal/mol, respectively, and the intensities and the frequencies of the processes are very close (see Fig. 7 of Ref. [43]). Such coincidences are highly improbable for so different slip processes. One has to prefer the hypothesis in the framework of which it is the coincidence that one is to expect. Our hypothesis of the chain diffusion through crystallites gives such result. Indeed, the lamellae are connected by through-pass chains in all directions. Therefore the direction of oscillations does not play any role if only the amorphous layers are not directly affected by the cyclic motion. This is the case for the mentioned directions (and not the case for any other direction).

Our assignment is confirmed by the fact that in single crystals there is only mechanical  $\alpha_2$  process [15] (possessing high activation energy), and one cannot observe mechanical processes corresponding to both types of chain diffusion through crystallites. Indeed, monocrystals in such a sample are not connected by through-pass chains, and even though the point defects can very rarely appear at the ends of the chains or in the loops their presence cannot be detected mechanically.

### 5.3. Dynamic mechanical experiment: diffusion of loose and entangled chains in ultradrawn PE films

Let us examine the properties of the dynamic mechanical  $\alpha$  process in a dry gel film on its drawing with draw ratios  $\lambda$

up to 400 [2]. The drawing was performed at temperature  $135^\circ\text{C}$  (the melting temperature of the gel film is  $140^\circ\text{C}$ ). The dry gel film has a very anisotropic structure. Its lamellae are oriented so that their  $c$ -axes are perpendicular to the film surface. In the process of drawing of the dry gel film the lamellae first re-orient so that the  $c$ -axes coincide with the drawing direction and then (after  $\lambda = 20$ ) re-form into fibrillar structures [1].

The dynamic mechanical  $\alpha$  process appears to consist of two  $\alpha_1$  and  $\alpha_2$  processes. As the draw ratio increases, the central frequency of both  $\alpha$  processes drops (Figs. 6 and 11 of Ref. [2]) from about  $10^2$ – $10^3$  Hz ( $\lambda = 1$ ) to less than 10 Hz ( $\lambda = 400$ ) at temperature  $65^\circ\text{C}$  ( $1000/T = 2.96/\text{K}$ ). It corresponds to our hypothesis on the mechanism of the process. Indeed, in the drawn film, the amorphous fraction becomes more and more restricted in mobility, the pulls at chains in crystallites become more and more rare and the central frequency of the H-diffusion process drops correspondingly.

More interesting is that the activation energy of the  $\alpha_1$  process lowers from 26 to 19 kcal/mol when  $\lambda$  increases from 1 to 100, and beyond this value the energy levels off (see Table 3 repeating Table II from Ref. [2]). Still more interesting is that in the films having draw ratio more than 20, the  $\alpha_2$  process has activation energies of the H-process (see Table 3). At the same time, as the draw ratio increases, the intensity of the  $\alpha_2$  process decreases. At the draw ratio 400 the  $\alpha_2$  process is absent, and the  $\alpha_1$  process alone is seen in the temperature range where both the processes were present for the lower draw ratios.

These facts have never been accounted for. We dare to offer some speculations which need further experimental examination. As we have found out before, the H-diffusion manifests itself mechanically as the  $\alpha_1$  process – in semicrystalline samples. We think that in such samples the  $\alpha_2$  process (which has activation energy 38.9 kcal/mol in dry gel films) is connected with motion of lamellae or blocks of these lamellae. After the draw ratio exceeds 20, this  $\alpha_2$  process leaves the available temperature range or, more probably, disappears together with the distinct old lamellae in the sample. Exactly at this point, the  $\alpha_1$  process bifurcates into the new  $\alpha_2$  and  $\alpha_1$  processes. We think that the reason is that chains in amorphous fraction of the drawn film may be of two different types. Some of the chains remain loose and the others become tense after drawing because of entanglements. The first ones are responsible for the new  $\alpha_2$  process which exactly corresponds to the dielectric  $\alpha$  process in common samples. The contribution of the loose chains into the  $\alpha_2$  process has to lower because at higher

Table 3  
Activation energies (in kcal/mol) of the  $\alpha_1$  and  $\alpha_2$  mechanical processes in PE ultradrawn gel films [2]

Draw ratio	$\alpha_1$	$\alpha_2$
1	26.3	38.9
20	<b>23.9</b>	28.2
60	20.5	24.8
100	19.1	<b>23.6</b>
400	18.9	–

draw ratios these chains have to be included into fibrillae in the process of drawing. So the  $\alpha_2$  process must disappear at some draw ratio – and it does. In contrast with it, if a through-pass chain is somehow fastened it cannot build into a fibril. The cooling fixes some tension in the disordered parts of these chains. The tension is more at higher draw ratios. This stored energy is used in creation of the smooth twist–tension defects and therefore the activation energy of the  $\alpha_1$  process lessens. Because there are evident physical restrictions on the value of this tension, the activation energy of the  $\alpha_1$  process levels off.

## 6. Conclusion

The H-diffusion process can be observed in dielectric or NMR measurements on common samples with loose enough amorphous fraction, but in samples where the genuine rubber-like amorphous fraction is absent (in fibers or single crystals) or restricted in mobility (in ultradrawn films or in electron beam irradiated samples) the frequency of the process becomes very low and it can be observed only in mechanical experiments where it shows up as the cheapest and the fastest of the mechanical  $\alpha$  processes. In ultradrawn films the H-process seems to bifurcate and the activation energy of the faster process decreases because of tension in the disordered fraction.

The L-diffusion process is available for observation in NMR experiments on fibers and single crystals. It has never been reported in dielectric experiments probably because of technical difficulties arising at low frequencies. The H-process has never been investigated dielectrically in ultradrawn films. Both gaps in experimental data are very unfortunate. The shape of dielectric loss curve provides information about statistics of the flips of the dipoles. As we have seen, for the H-process this statistics is the statistics of thermal pulls at chains in crystallites. For the L-process, this statistics is the statistics of fluctuations of the boundaries of crystalline regions. All one knows is that the H-process has a ‘quasi-Debye’ dielectric loss curve [12,10,13], which means a ‘quasi-Poisson’ statistics of the pulls, and the reason why it is not a Poisson one is yet unclear. Dielectric experiments on ultradrawn films could shed light on the problem. About the statistics of the L-diffusion process (which is much more interesting) one knows nothing – to the best of our knowledge. So the well known process of chain diffusion between amorphous and crystalline fractions in polymers may be worth for further investigation.

## Acknowledgements

The authors thank the Russian Foundation for Basic Research (awards 04-03-32119 and 05-03-32241) for financial support. Numerical calculations were carried out in the Joint Supercomputer Center of the Russian Academy of Sciences. One of the authors (E.A.Z.) acknowledges substantial help of the Russian Science Support Foundation. We also thank Prof. A. Arinstein for helpful discussions.

## References

- [1] Hu W-G, Schmidt-Rohr K. *Acta Polym* 1999;50:271.
- [2] Matsuo M, Sawatari C, Ohhata T. *Macromolecules* 1988;21:1317.
- [3] Schmidt-Rohr K, Spiess HW. *Macromolecules* 1991;24:5288.
- [4] Klein PG, Robertson MB, Driver MAN, Ward IM, Parker KJ. *Polym Int* 1998;47:76.
- [5] Kuwabara K, Kaji H, Tsuji M, Horii F. *Macromolecules* 2000;33:7093.
- [6] Hu W-G, Boeffel C, Schmidt-Rohr K. *Macromolecules* 1999;32:1611.
- [7] Schmieder K, Wolf K. *Kolloid Z Z Polym* 1953;134:157.
- [8] Mikhailov GP, Lobanov AN, Sazhin BI. *Zh Tekh Fiz* 1954;24:1553; Mikhailov GP, Kabin SP, Sazhin BI. *Zh Tekh Fiz* 1955;25:590; Mikhailov GP, Kabin SP, Krylova TA. *Zh Tekh Fiz* 1957;27:2050 [in Russian].
- [9] Oakes WG, Robinson DW. *J Polym Sci* 1954;14:505.
- [10] Ashcraft CR, Boyd RH. *J Polym Sci Polym Phys Ed* 1976;14:2153.
- [11] Boyd RH, Yemni T. *Polym Eng Sci* 1979;14:1023.
- [12] Ishida Y, Yamafuji K. *Kolloid Z Z Polym B* 1965;202(H1):26.
- [13] Sayre JA, Swanson SR, Boyd RH. *J Polym Sci Polym Phys Ed* 1978;16:1739.
- [14] Boyd RH. *Macromolecules* 1984;17:903.
- [15] Manabe S, Sakoda A, Katada A, Takayanagi M. *J Macromol Sci Phys B* 1970;4:161.
- [16] Nakayasu H, Markovitz H, Plazek DJ. *Trans Soc Rheol* 1961;5:261.
- [17] McCrum NG, Morris EL. *Proc R Soc London Ser A* 1964;281:258.
- [18] Ogita T, Yamamoto R, Suzuki N, Matsuo M. *Polymer* 1991;32:822.
- [19] Ohta Y, Yasuda H. *J Polym Sci Part B Polym Phys* 1994;32:2241.
- [20] Hoffman JD, Williams G, Passaglia E. *J Polym Sci C* 1966;14:173.
- [21] Buckley CP, McCrum NG. *J Mater Sci* 1973;8:928.
- [22] Takayanagi M. Molecular basis of transition and relaxation. In: Meier DJ, editor. *Midland macromolecular monographs*, vol. 4. London: Gordon and Breach; 1978. p. 117–65.
- [23] McCrum NG. Molecular basis of transition and relaxation. In: Meier DJ, editor. *Midland Macromolecular Monographs*, vol. 4. London: Gordon and Breach; 1978. p. 167–91.
- [24] Saito N, Okano K, Iwayanagi S, Hideshima T. In: Seitz F, Turnbull D, editors. *Solid state physics*, vol. 14. New York: Academic Press; 1963. p. 453–68.
- [25] Kawai H, Suehiro S, Kyu T, Shimomura A. *Polym Eng Rev* 1983;3:109.
- [26] Men Y, Rieger J, Endeler H-F, Lilge D. *Macromolecules* 2003;36:4689.
- [27] Mano JF, Sousa RA, Reis RL, Cunha AM, Bevis MJ. *Polymer* 2001;42:6187.
- [28] Kolesov I, Androsch R, Radusch H-J. *Macromolecules* 2005;38:445.
- [29] Reneker DH, Fanconi BM, Mazur J. *J Appl Phys* 1977;48:4032.
- [30] Mansfield MS, Boyd RH. *J Polym Sci Polym Phys Ed* 1978;16:1227.
- [31] Mansfield MS. *Chem Phys Lett* 1980;69:383.
- [32] Reneker DH, Mazur J, Colson JP, Snyder RG. *J Appl Phys* 1980;51:5080.
- [33] Xiao Y, Yan L, Zhang P, Zhu N, Chen L, He P, et al. *J Appl Polym Sci* 2006;100:4835.
- [34] Matsuo M, Bin Y, Xu Ch, Ma L, Nakaoki T, Suzuki T. *Polymer* 2003;44:4325.
- [35] Zerbi G, Longhi G. *Polymer* 1988;29:1827.
- [36] Manevitch LI, Ryvkina NG. In: Hsieh RKT, editor. *Mechanical modeling of new electromagnetic materials*. Elsevier; 1990. p. 155–61.
- [37] Zhang F. *Phys Rev E* 1997;56:6077.
- [38] Skinner JL, Wolynes PG. *J Chem Phys* 1980;73:4015, 4022.
- [39] Skinner JL, Park YH. *Macromolecules* 1984;17:1735.
- [40] Wahlstrand KJ. *J Chem Phys* 1985;82:5247; Wahlstrand KJ, Wolynes PG. *J Chem Phys* 1985;82:5259; Wahlstrand KJ. *Polymer* 1988;29:256, 263.
- [41] Zubova EA, Balabaev NK, Manevitch LI. *Zh Eksp Teor Fiz* 2002;121:884 [J Exp Theor Phys 2002;94:759].
- [42] Reneker DH, Mazur J. *Polymer* 1982;23:401.
- [43] Zhou H, Wilkes GL. *Macromolecules* 1997;30:2412.
- [44] Weiner SJ, Kollman PA, Case DA, Singh UC, Ghio C, Alagona G, et al. *J Am Chem Soc* 1984;106:765.
- [45] Berendsen HJC, Postma JPM, Gunsteren WF, DiNola A, Haak JR. *J Chem Phys* 1984;81:3684.



- [46] Lemak AS, Balabaev NK. *Mol Simul* 1995;15:223.
- [47] Lemak AS, Balabaev NK. *J Comput Chem* 1996;17:1685.
- [48] Allen MP, Tildesley PJ. *Computer simulation of liquids*. Oxford: Clarendon; 1987.
- [49] Zhang F. *Phys Rev B* 1999;59:792.
- [50] Zubova EA, Balabaev NK, Manevitch LI, Tsygurov AA. *Zh Eksp Teor Fiz* 2000;118:592 [*J Exp Theor Phys* 2000;91:515].
- [51] Reneker DH, Mazur J. *Polymer* 1988;29:3.
- [52] Mowry SW, Rutledge GC. *Macromolecules* 2002;35:4539.
- [53] Graff MS, Boyd RH. *Polymer* 1994;35:1797.
- [54] The results on MD simulation of a purely amorphous PE sample and a sample including both amorphous and crystalline fractions will be published later.
- [55] Mano JF. *Macromolecules* 2001;34:8825.

Author's personal copy